Segmentation of Individual Renal Cysts from MR Images in Patients with Autosomal Dominant Polycystic Kidney Disease

Kyungsoo Bae, Bumwoo Park,* Hongliang Sun,* Jinhong Wang,* Cheng Tao,* Arlene B. Chapman,† Vicente E. Torres,‡ Jared J. Grantham,§ Michal Mrug,‖ William M. Bennett,¶ Michael F. Flessner,** Doug P. Landsittel,†† and Kyongtae T. Bae,* for the Consortium for Radiologic Imaging Studies of Polycystic Kidney Disease (CRISP)*

*Department of Radiology and ††Department of Internal Medicine, University of Pittsburgh School of Medicine, Pittsburgh, Pennsylvania; †Department of Internal Medicine, Emory University School of Medicine, Atlanta, Georgia; ‡Department of Internal Medicine, Mayo College of Medicine, Rochester, Minnesota; §Department of Internal Medicine, Kansas University Medical Center, Kansas City, Kansas; ‖Division of Nephrology, University of Alabama, Birmingham, Alabama; ¶Legacy Good Samaritan Hospital, Portland, Oregon; and **National Institute of Diabetes and Digestive and Kidney Diseases, National Institutes of Health, Bethesda, Maryland

Correspondence: Dr. Kyongtae T. Bae, Department of Radiology, University of Pittsburgh School of Medicine, Presbyterian South Tower, Room 3950, 200 Lothrop Street, Pittsburgh, PA 15213. Email: baek@upmc.edu

Summary

Objective To evaluate the performance of a semi-automated method for the segmentation of individual renal cysts from magnetic resonance (MR) images in patients with autosomal dominant polycystic kidney disease (ADPKD).

Design, setting, participants, & measurements This semi-automated method was based on a morphologic watershed technique with shape-detection level set for segmentation of renal cysts from MR images. T2-weighted MR image sets of 40 kidneys were selected from 20 patients with mild to moderate renal cyst burden (kidney volume < 1500 ml) in the Consortium for Radiologic Imaging Studies of Polycystic Kidney Disease (CRISP). The performance of the semi-automated method was assessed in terms of two reference metrics in each kidney: the total number of cysts measured by manual counting and the total volume of cysts measured with a region-based thresholding method. The proposed and reference measurements were compared using intraclass correlation coefficient (ICC) and Bland-Altman analysis.

Results Individual renal cysts were successfully segmented with the semi-automated method in all 20 cases. The total number of cysts in each kidney measured with the two methods correlated well (ICC, 0.99), with a very small relative bias (0.3% increase with the semi-automated method; limits of agreement, 15.2% reduction to 17.2% increase). The total volume of cysts measured using both methods also correlated well (ICC, 1.00), with a small relative bias of <10% (9.0% decrease in the semi-automated method; limits of agreement, 17.1% increase to 43.3% decrease).

Conclusion This semi-automated method to segment individual renal cysts in ADPKD kidneys provides a quantitative indicator of severity in early and moderate stages of the disease.

Clin J Am Soc Nephrol 8: 1089–1097, 2013. doi: 10.2215/CJN.10561012

Introduction

Autosomal dominant polycystic kidney disease (ADPKD) begins in relatively few renal tubules that expand progressively to overwhelm the residual non-cystic functioning parenchyma in severe cases (1). The appearance and growth of renal cysts are strongly associated with disease progression to renal insufficiency (2).

The Consortium for Radiologic Imaging Studies of Polycystic Kidney Disease (CRISP) was established to collect magnetic resonance imaging (MRI), renal function, and biomarker data relevant to disease progression in affected individuals in the early course of the disease (3). CRISP findings indicate that kidney volume measurements from MRI are more sensitive than renal-function measures in assessing yearly progression of the disease (4). CRISP also revealed that the number of cysts detectable by MRI increases with age and that renal morphologic (and associated phenotypical and clinical) differences between *PKD1* and *PKD2* genotypes are likely because more cysts develop earlier with *PKD1*, not because the cysts grow faster (5).

Recently, we found that MRI detects a relatively small fraction of the total cysts in a polycystic kidney (6). Of note, the cysts below MRI detection (<1.0 mm diameter) continue to expand and eventually become visible on MRI; the increase in number indicates disease progression. However, these studies were based on the manual counting of renal cysts. To further explore the relationship of cyst number and disease severity, it is necessary to standardize cyst counting from the entire three-dimensional MR image data set. Although the manual segmentation method (manual delineation of the borders) of individual cysts from the kidney is straightforward, it is laborious, time-consuming, and subject to observer error and bias. Consequently, in this study we developed

a semi-automated method to segment and count the individual renal cysts from MR images.

Materials and Methods

The study protocol for CRISP (clinical trials registration number, NCT01039987; registration date, December 23, 2009) has been previously described (3,4,7) and was approved by the institutional review board at each participating clinical center. Informed consent was obtained from all CRISP participants. The clinical and research activities being reported are consistent with the Principles of the Declaration of Istanbul, as outlined in the "Declaration of Istanbul on Organ Trafficking and Transplant Tourism."

Participants and MR Imaging

CRISP was launched in 1999 to acquire prospective, multiyear, longitudinal measurements of renal and renal cyst volumes in a large cohort of patients with ADPKD who had relatively intact renal function. The CRISP cohort consists of 241 patients with ADPKD age 15–46 years with relatively intact renal function. Detailed descriptions of the CRISP study protocol, the clinical characteristics of the cohort, and the baseline characteristics have been published previously (3,4,7). In brief, the MRI protocol for CRISP was standardized and implemented in 1.5-T MRI scanners. In each participant, a phased-array surface coil was positioned with its center over the inferior costal margin, estimated as the upper margin of the kidney. The field of view was maintained between 30 and 35 cm. The kidneys were imaged at 3-mm fixed slice thickness in the coronal plane using the T2-weighted single-shot fast spin-echo sequence with fat saturation, as well as three-dimensional spoiled gradient interpolated T1-weighted images without fat saturation and during breathholds (3).

We stratified participants into three groups according to their kidney size (combined right and left kidney volumes $\leq$750, 750–1500, $>$1500 ml). This kidney-size group stratification is the same scheme used in previous CRISP studies (4,7). Using a random-number generator, we randomly chose 10 patients each from the three groups (mild, moderate, and severe cyst burden) (Figure 1). Preliminary testing of the semi-automated method on the kidneys from the group with severe cyst burden revealed that successful segmentation of each individual cyst was tremendously laborious, requiring extensive manual editing (data not shown). Even manual counting of each cyst from this group (performed by a radiologist) proved to be very challenging. Because the major utility of cyst counts lies in the evaluation of disease progression in the earliest stages of the disease (before GFR has declined), we limited our study cohort to the 20 patients from the mild and moderate groups (7 male and 13 female patients; mean age, 30.8 years [range, 17–46 years]).

Manual Cyst Counting and Total Cyst Volume Measurements Using Region-based Method

The T2-weighted MR images of the abdomen from each of the 20 patients were reviewed and cropped to separate and generate images of the right and left hemi-abdomen. Each image set had the same voxel resolution as the original image set. From the cropped image set of the hemi-abdomen, the kidney boundary was detected and segmented using image editing software (Analyze, version 10.0; Mayo Clinic, Rochester, MN). The calyx and renal pelvis were carefully identified and excluded. Segmented kidneys from the three groups are shown in Figure 1.

The total number of cysts in each kidney was determined manually by a radiologist (K.S.B.). For counting cysts, we accepted circular and spheroid structures $\geq$2 mm in diameter whose signal intensities were close to that of spinal fluid. Reading through the sequential slices back and forth was required to identify each cyst, as well as to avoid overcounting cysts occupying more than one slice. To assure counting of each cyst only once, a radiologist marked each identified cyst by electronic marker using an in-house cyst-labeling program. At the initial slice, all identified cysts were flagged with red marks. At the next slice, carryover cysts were flagged with blue marks, whereas the newly identified cysts were labeled with red marks. The radiologist reviewed adjacent slices back and forward to ensure that every identified cyst in each slice was appropriately flagged and accounted for without missing any cyst (Figure 2A). When all cysts were manually marked over the entire set of kidney images, the total number of cysts flagged with red marks was automatically computed.

The total volume of cysts in each kidney was measured by a different radiologist (J.H.W.) using a region-based thresholding method (3,7). Cysts were brighter than the renal parenchyma on T2-weight images. Therefore, they could be measured by summing voxels with intensity values greater than those of the background renal parenchyma. On each renal MR image slice, a binary signal-intensity map was generated. This was done by determining a threshold signal intensity that visually distinguished the cyst and renal parenchymal regions. In the binary map, cysts that were brighter than renal parenchyma are represented as white regions, whereas the background renal parenchyma was designated as black regions (Figure 2B). By summing the pixels of white regions, the cystic area was measured in each slice. The total cyst volume was calculated from each set of contiguous images by summing the products of the areas measured and the slice thickness.

Semi-automated Cyst Segmentation

An overview of the semi-automated segmentation processes used in the study is presented in the flowchart shown in Figure 3. The segmentation program was implemented on ITK (Insight Toolkit, version 3.10.0) and Visual Studio C++ 2005. First, from a set of segmented kidney images, cyst regions (cyst candidate region) that were brighter than renal parenchyma regions were obtained with a K-means clustering method (8). A connected components analysis was applied to the cyst candidate region to extract and label candidates for individual cyst regions. To further break apart individual cysts from connected components analysis regions, a level-set image was generated with the Fast Marching method (9). In a separate pathway, a cyst edge potential image was created from the initial segmented kidney image set by applying multiple filters, including the anisotropic diffusion filter, the gradient magnitude filter, and the sigmoid filter (10). The cyst edge potential image and the level-set image were

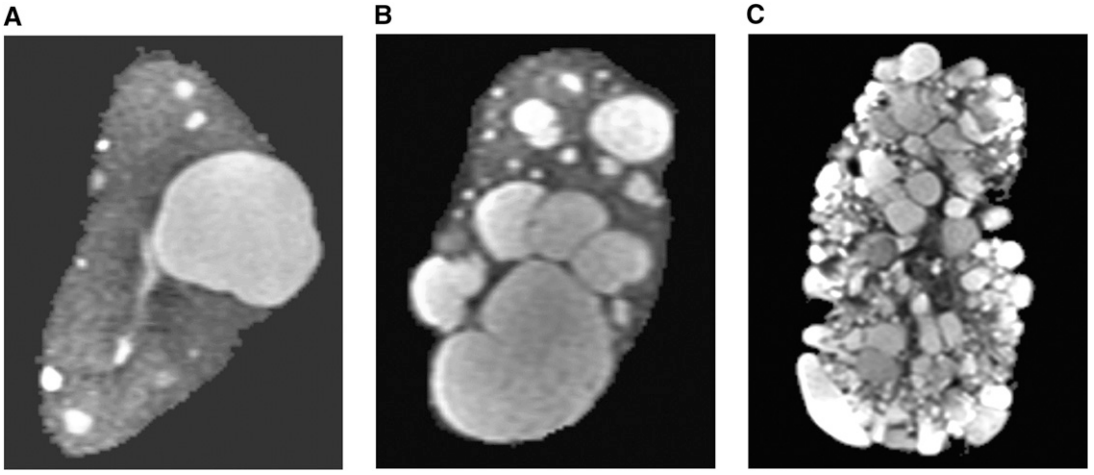

Figure 1. | T2-weighted coronal magnetic resonance images illustrating three groups of cyst-burden severity. (A) In the mild cyst-burden group, cysts are scattered and discretely defined by surrounding renal parenchyma. Most cysts are well separated without touching each other. (B) In the moderate cyst-burden group, the number and volume of cysts are greater than those of the mild cyst-burden group. Most cysts remain discernible and surrounded by renal parenchyma, although some neighboring cysts may share borders. (C) In the severe cyst-burden group, kidney tissue is almost completely replaced by innumerable cysts, with little discernible renal parenchyma. Segmentation of individual cysts by the computer is extremely challenging in this group.

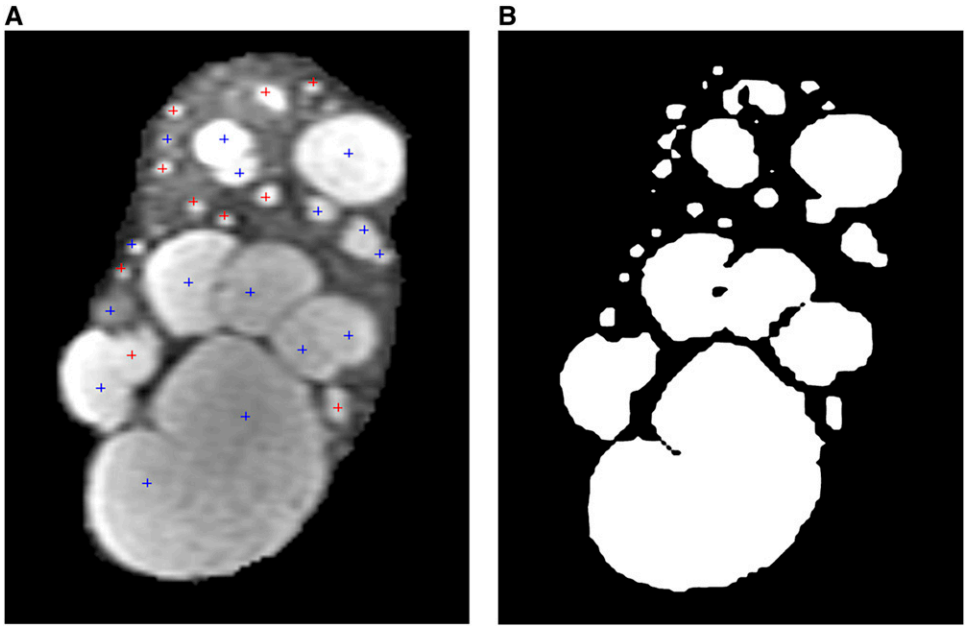

Figure 2. | Magnetic resonance images from a 41-year-old man with autosomal dominant polycystic kidney disease and moderate cyst burden (corresponding to Figure 1B). The images illustrate an intermediate step of (A) manual cyst counting and (B) total cyst volume measurement using a region-based thresholding method. (A) The manual counting method was performed using an in-house cyst-labeling computer program. At the initial slice, a radiologist manually flagged all identified cysts by electronic marker (red marks). At the next slice, the carryover cysts are flagged with blue marks, whereas newly identified cysts are labeled in red marks. After all cysts were manually marked over the entire set of kidney images, the total number of cysts flagged with red marks is automatically computed. (B) On each slice of kidney MR images, a binary signal-intensity map is generated by determining a threshold signal intensity that visually distinguishes the cyst and renal parenchyma regions. In the binary map, cysts that are brighter than renal parenchyma are represented as white regions, whereas the background renal parenchyma is designated as black regions.

compared with additional cyst candidates. A shape detection level set algorithm was applied to individual cyst candidates to identify a seed point of each cyst (11). The process of erosion of cyst candidates and identification of cyst seed points was iterated until there was no further erosion or gain of additional cyst candidates. The final image data set with individual cysts marked by their seed points was denoted as a marker image.

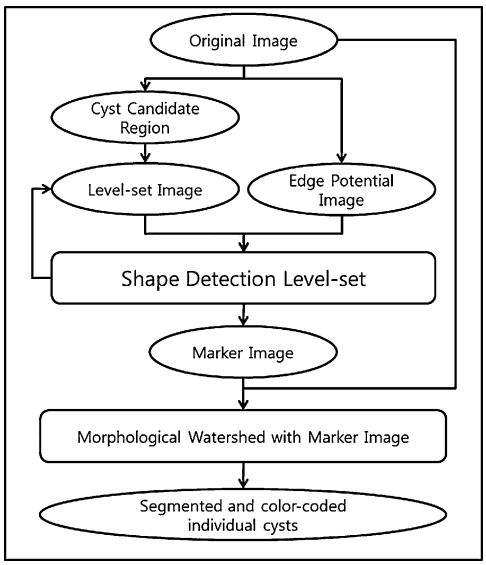

Figure 3. | Overview of the semi-automated segmentation processes of individual cysts.

A morphologic watershed algorithm (12) was applied to the marker and initial segmented kidney image sets to segment and identify individual cysts. While reviewing the initial segmentation result, the observer could revise cystic structures that were deemed to be incomplete or had been erroneously segmented by the placement of additional or revised seeds. This iterative reseeding-segmentation process could be repeated until the segmented outcome was satisfactory. The segmented individual cysts were numbered, color-coded, and volumetrically measured (Figure 4).

Statistical Analyses

The performance of the semi-automated segmentation method was evaluated and compared with the manual method in terms of the total number and total volume of individual cysts in each kidney. These reference measurements were derived using the approach illustrated in Figure 2. The segmentation outcome of each individual cyst could not be assessed because it was not available by the reference methods. The total cyst number and cyst volume measurements in each kidney between the semi-automated and reference methods were compared by means of intraclass correlation coefficient (ICC) (13) and corresponding confidence intervals. In addition, Bland-Altman analysis (using natural log-transformed data to achieve more constant variance) was used to visually assess systemic differences (14) and estimate bias and limits of agreement (LOAs). To interpret in the original scale, we report the relative bias and LOAs as a percentage increase or decrease (because back-transforming a difference in logarithms gives a ratio, not an absolute difference). The statistical analyses were performed in Stata software, version 11 (Stata Corp., College Station, TX); Bland-Altman plots were created using the batplot command.

Results

The total numbers of cysts in kidneys measured with the semi-automated segmentation method ranged from 12 to 242 (mean, 91), and total numbers with the manual counting method were 11–256 (mean, 90) (Table 1). The mean difference in the total numbers of cysts ± SD (*i.e.*, the manual − the semi-automated segmentation count) was −0.90±12.4 (interquartile range, −9.5 to 6.5). The two methods correlated well (ICC, 0.99; 95% confidence interval CI, 0.98 to 1.00) (Figure 5A). Bland-Altman analysis for the two methods in counting cyst number showed a very small estimated bias; there was a relative bias of a 0.3% increase in the semi-automated over the manual method, with 95% LOAs spanning a 15.2% decrease to a 17.2% increase (Figure 5B displays log-transformed values). Differences showed a relatively even spread around 0 across the range of average counts. All 40 points fell within the limits of agreement.

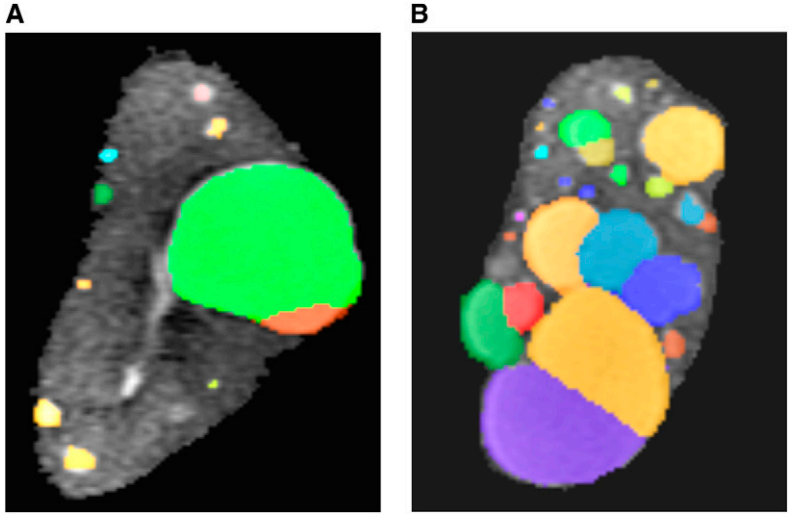

Figure 4. | Individual renal cysts segmented and color-coded using the semi-automated method. (A) Magnetic resonance image from an 18-year-old man with autosomal dominant polycystic kidney disease (ADPKD) in the mild cyst-burden group (corresponding to Figure 1A) and (B) 41-year-old man with ADPKD and moderate cyst burden (corresponding to Figure 1B).

Table 1. Total counts and total volumes of cysts in each kidney measured with the semi-automated segmentation versus two other methods

Patient	Total Cyst Count (*n*)				Total Cyst Volume (ml)			
	Manual		Semi-automated		Region-based		Semi-automated	
	Left	Right	Left	Right	Left	Right	Left	Right
1	73	76	77	73	110	30	90	24
2	72	74	78	79	41	78	33	78
3	56	54	64	60	80	226	75	207
4	63	73	67	65	21	72	18	59
5	65	64	63	62	30	32	21	23
6	120	98	128	92	986	298	973	295
7	144	111	156	130	153	153	171	178
8	82	73	81	67	53	19	50	14
9	26	27	25	27	47	92	47	77
10	64	42	57	41	21	156	15	159
11	63	82	67	75	122	80	114	85
12	62	57	72	55	950	1379	930	1409
13	84	122	98	119	133	86	131	97
14	63	52	58	52	47	46	44	36
15	82	67	75	64	20	9	16	7
16	48	46	48	40	8	11	10	9
17	157	160	175	165	94	374	88	358
18	230	256	242	228	472	583	410	538
19	17	11	16	12	2	53	2	55
20	241	250	239	233	497	565	479	519

The total volumes of renal cysts measured with the semi-automated method (which corresponded to the sum of the volumes of individual cysts in each kidney) ranged from 2 to 1409 ml (mean, 199 ml); total volumes with the region-based method ranged from 2 to 1379 ml (mean, 206 ml) (Table 1). The mean difference in the total cyst volume (*i.e.*, the region-based volume − the semi-automated segmentation volume) was 14.2±29.7 ml (interquartile range, 0.6–20 ml). The correlation between the two measurement methods was excellent (ICC, approximately 1.00; the lower limit of the 95% confidence interval was also approximately 1.00) (Figure 6A). Bland-Altman analysis for the total cyst volume with the two methods showed an estimated bias of a 9% decrease in the semi-automated method (95% LOAs were 17.1% increase to 43.3% decrease; see Figure 6B for the plot of log-transformed data). Differences again showed a relatively even spread around the estimated mean difference across the range of average volumes; 95% of the 40 points fell within the LOAs.

The ICCs and Bland-Altman analysis for the total cyst counts and volumes were also performed separately for the left and right kidneys and summing over both kidneys; ICCs and Bland-Altman plots showed very similar results, with the relative bias being no more than 2.2% for cyst counts and no more than 9.1% for volumes, with ICCs of 0.99–1.00.

Discussion

In a recent landmark controlled clinical trial (15), tolvaptan reduced the rate of increase in total kidney volume by 49% and slowed the decrease in GFR by 31%. Annual MRI measurements were used to quantify renal volume in that study, which included patients with ADPKD who had relatively large kidneys and mild to moderately severe reductions in GFR at baseline. Determining the effect of therapeutic candidates such as tolvaptan in patients with less advanced disease is more difficult because the inherent small error of kidney volume measurements is proportionately larger in relation to the annual increase in total kidney volume (15). An increase in kidney volume is due to the growth of extant cysts and the addition of new ones. Because evidence from CRISP indicated that total cyst burden and total cyst volume are also associated with the decline in GFR, we decided to develop a method to quantify these measures so that indicators of disease progression could be determined in the earliest stages of the disease.

In a previous study (6), we used a labor-intensive manual method to determine the number and volumes of individual cysts in eight kidneys in the CRISP cohort. Although we counted the total number of cysts in the kidneys, we measured cyst volume in only a subset. To our knowledge, no other study has reported the segmentation of individual renal cysts in a way that facilitates measurement of the number, size, and topologic distribution of all visible cysts within the kidneys. Two recent studies (5,16) estimated the number of renal cysts in ADPKD kidneys by manual counting using only a middle section rather than the entire volume of MR images. The method described in the current report performed well in kidneys with mild and moderate cystic burdens but not in those in which parenchyma was largely replaced by cysts.

The semi-automated cyst segmentation method was evaluated by the manual counting of renal cysts and the region-based thresholding method for measuring total cyst volume. The semi-automated and corresponding reference methods showed excellent ICCs, with a relatively small

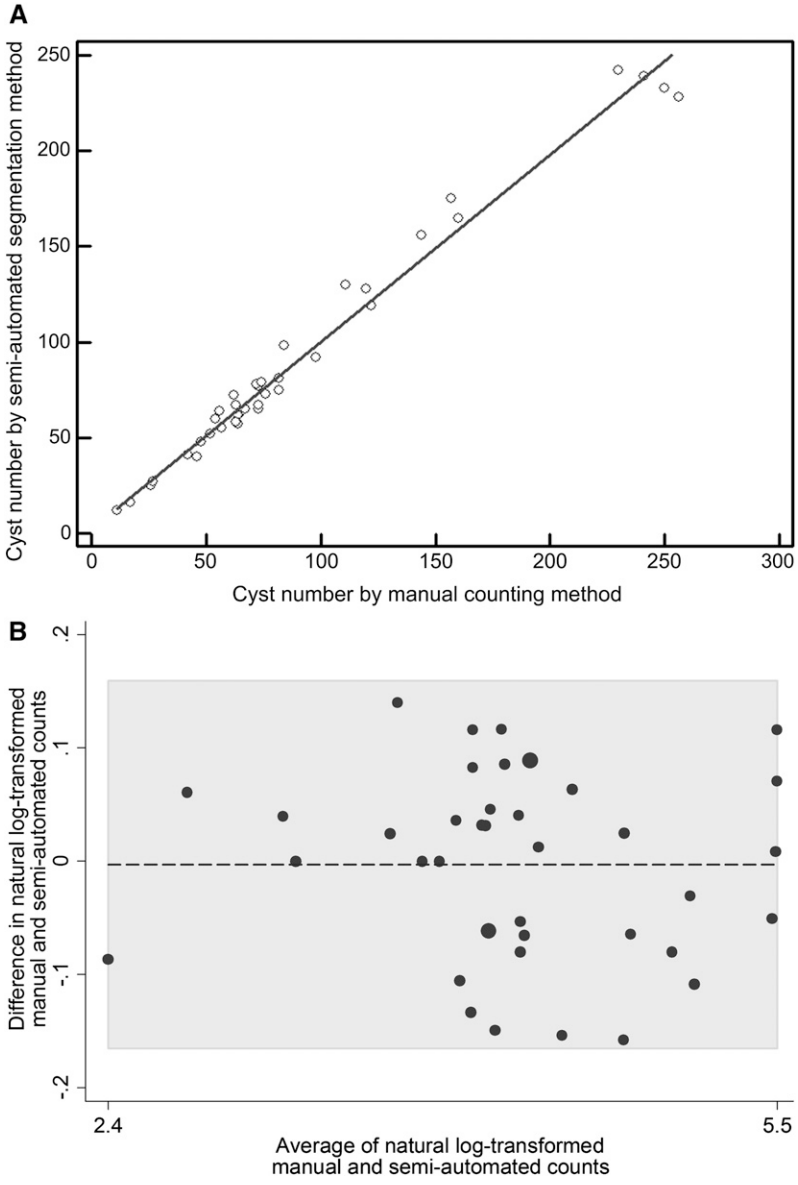

Figure 5. | Comparison of the manual and semi-automated renal cyst counts in 20 patients. (A) Scatter plot of the manual versus semi-automated renal cyst counts in 20 patients. Line shows line of regression fitted using a least-squares method (with coefficient of 0.98; R^2=0.98; P<0.001). (B) Bland-Altman plot for the manual versus semi-automated renal cyst counts.

bias and narrow LOAs in the Bland-Altman analysis. Because there is no specific reference measurement against which to compare each individual renal cyst, we could not assess the accuracy of segmentation of individual cysts.

There was a small systemic underestimation (9.0%) of total cyst volume measurements with the semi-automated method compared with the region-based thresholding method. This discrepancy was probably a result of the intrinsic technical differences between the two methods. In the region-based thresholding method, the cyst area is differentiated from the background renal parenchyma and computed by thresholding of signal intensity over the entire kidney region. Hence, even a single bright pixel may be included in the computation of cyst area. On the other hand, the semi-automated method requires the minimum size of a cyst to be a cluster of bright pixels 2–3 mm in diameter. An isolated single bright pixel or microcyst is not considered to be a cyst in the semi-automated program because a tiny area cannot be differentiated from background noisy renal parenchyma. Therefore, the total cyst volume measured by the semi-automated method is expected to be smaller than that measured by the region-based thresholding method. This relative difference between the two methods in the estimation of total cyst volume would be more pronounced in kidneys with smaller cyst burdens. This is evidenced by the Bland-Altman analysis; when this analysis was performed only for the kidneys whose total cyst volume is >30 ml, the bias was considerably reduced to 4.8% from 9.0%. Furthermore, we postulate that the use of more strict thresholds in the region-based thresholding method may lead to smaller total cyst volumes matching closer to those measured with the semi-automated method.

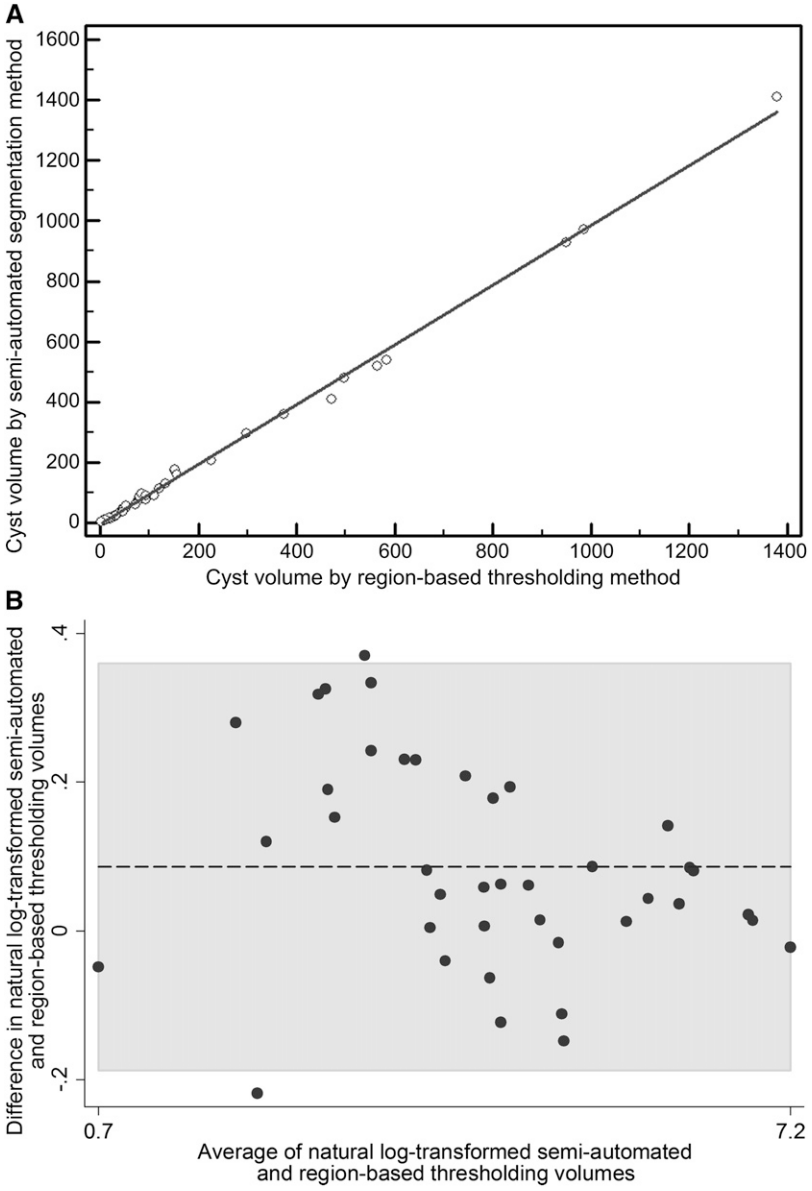

Figure 6. | **Comparison of the semi-automated and region-based thresholding measurements of total cyst volume in kidneys.** (A) Scatter plot of the semi-automated versus region-based thresholding measurements of total cyst volume in kidneys. Line shows line of regression fitted using a least-squares method (with coefficient of 0.99; R^2=1.00; P<0.001). (B) Bland-Altman plot for the semi-automated versus region-based thresholding measurements of total cyst volume in kidneys.

Both the semi-automated method and region-based thresholding method require a prior segmentation of kidney from abdominal MR images. This operation was carried out semi-automatically in each slice of MR images by placing a seed point over the kidney area. The segmented kidney boundary is further refined and edited by an operator to correct segmentation errors and exclude renal hila and the extra-parenchymal collecting system. A fully automated method would be preferred for the segmentation of both kidney and individual renal cysts, such as the one used for normal kidneys (17,18). Unfortunately, owing to the complex structure of cystic kidneys and variations in MR signal characteristics, completely automatic segmentation must await further technical development.

The structure and MR signal intensities of kidneys with many cysts become increasingly heterogeneous as the disease progresses (19). In advanced ADPKD, cysts are innumerable, touching and inseparable from each other because there is no discernible background renal parenchyma. The segmentation of individual cysts in these advanced ADPKD cases requires the labor-intensive manual editing of each cyst (even after an initial segmentation performed by the computer) and is impractical. Consequently, the semi-automated method described here will probably find greatest usefulness in the quantitative analysis of cyst number and total cyst volume in the early stages of ADPKD. In young children, for example, the kidneys may be only marginally enlarged, making relatively

small changes in total kidney volume difficult to detect over a period of a few months or a year. On the other hand, total cyst number and total cyst volume determined by the semi-automated method would probably show significant changes, as we observed in a previous study using a manual segmentation method (6).

This study has several limitations. First, as noted above, our method is limited to patients with relatively mild to moderate ADPKD. Second, we analyzed and segmented cysts that were bright on T2-weighted MR images. Some complex and hemorrhagic cysts may appear as gray or dark signals on T2-weighted images. The identification of these cysts requires a careful visualization and comparison on both T1- and T2-weighted images. With T2-weighted images alone, they cannot be identified or segmented by any of the three methods (manual, semi-automated, or region-based thresholding) used in the study. Fortunately, these complex cysts are relatively uncommon in kidneys with mild to moderate cystic burdens, although their prevalence increases with disease severity. Third, microscopic cysts that are "invisible" by MRI cannot be segmented. A recent study (6) demonstrated that a vast number of microscopic cysts present in adult ADPKD kidneys remain undetected by clinically available imaging modalities. However, the collective volume of these microscopic cysts is quantitatively insignificant compared with the overall kidney size. Fourth, even though the segmentation process is semi-automated, manual editing may still be required after the initial segmentation of individual cysts by the computer. When renal cysts are not segmented automatically by the program, a radiologist must edit them by manually drawing their borders on MR images, adding a new seed point to segment an excluded cyst, or deleting a seed point to remove an incorrectly segmented structure.

In conclusion, we have developed a semi-automated method to segment individual renal cysts in ADPKD kidneys with mild to moderate cystic burdens. This method may help determine the extent and rate of disease progression in children and adults in the early stages of ADPKD.

Acknowledgments

The investigators are indebted to the radiologists, radiology technologists, imaging engineering staff, and study coordinators in CRISP.

CRISP is supported by cooperative agreements from the National Institute of Diabetes and Digestive and Kidney Diseases of the National Institutes of Health (DK056943, DK056956, DK056957, DK056961), the National Center for Research Resources General Clinical Research Centers at each institution (RR000039, Emory University; RR00585, Mayo College of Medicine; RR23940, Kansas University Medical Center; RR000032, University of Alabama at Birmingham), and the National Center for Research Resources Clinical and Translational Science Awards at each institution (RR025008, Emory; RR024150, Mayo College of Medicine; RR033179, Kansas University Medical Center; RR025777 and UL1TR000165, University of Alabama at Birmingham; RR024153 and UL1TR000005, University of Pittsburgh School of Medicine).

Disclosures

A.B.C. and J.J.G. are consultants to Otsuka Corp, and V.E.T. received research support from Otsuka Corp. M.M. is a consultant to Otsuka Corp and Alexion Pharmaceuticals.

References

1. Wilson PD: Polycystic kidney disease. *N Engl J Med* 350: 151–164, 2004
2. Chapman AB, Bost JE, Torres VE, Guay-Woodford L, Bae KT, Landsittel D, Li J, King BF, Martin D, Wetzel LH, Lockhart ME, Harris PC, Moxey-Mims M, Flessner M, Bennett WM, Grantham JJ: Kidney volume and functional outcomes in autosomal dominant polycystic kidney disease. *Clin J Am Soc Nephrol* 7: 479–486, 2012
3. Chapman AB, Guay-Woodford LM, Grantham JJ, Torres VE, Bae KT, Baumgarten DA, Kenney PJ, King BF Jr, Glockner JF, Wetzel LH, Brummer ME, O'Neill WC, Robbin ML, Bennett WM, Klahr S, Hirschman GH, Kimmel PL, Thompson PA, Miller JP; Consortium for Radiologic Imaging Studies of Polycystic Kidney Disease cohort: Renal structure in early autosomal-dominant polycystic kidney disease (ADPKD): The Consortium for Radiologic Imaging Studies of Polycystic Kidney Disease (CRISP) cohort. *Kidney Int* 64: 1035–1045, 2003
4. Grantham JJ, Torres VE, Chapman AB, Guay-Woodford LM, Bae KT, King BF Jr, Wetzel LH, Baumgarten DA, Kenney PJ, Harris PC, Klahr S, Bennett WM, Hirschman GN, Meyers CM, Zhang X, Zhu F, Miller JP; CRISP Investigators: Volume progression in polycystic kidney disease. *N Engl J Med* 354: 2122–2130, 2006
5. Harris PC, Bae KT, Rossetti S, Torres VE, Grantham JJ, Chapman AB, Guay-Woodford LM, King BF, Wetzel LH, Baumgarten DA, Kenney PJ, Consugar M, Klahr S, Bennett WM, Meyers CM, Zhang QJ, Thompson PA, Zhu F, Miller JP: Cyst number but not the rate of cystic growth is associated with the mutated gene in autosomal dominant polycystic kidney disease. *J Am Soc Nephrol* 17: 3013–3019, 2006
6. Grantham JJ, Mulamalla S, Grantham CJ, Wallace DP, Cook LT, Wetzel LH, Fields TA, Bae KT: Detected renal cysts are tips of the iceberg in adults with ADPKD. *Clin J Am Soc Nephrol* 7: 1087–1093, 2012
7. Bae KT, Zhu F, Chapman AB, Torres VE, Grantham JJ, Guay-Woodford LM, Baumgarten DA, King BF Jr, Wetzel LH, Kenney PJ, Brummer ME, Bennett WM, Klahr S, Meyers CM, Zhang X, Thompson PA, Miller JP; Consortium for Radiologic Imaging Studies of Polycystic Kidney Disease (CRISP): Magnetic resonance imaging evaluation of hepatic cysts in early autosomal-dominant polycystic kidney disease: The Consortium for Radiologic Imaging Studies of Polycystic Kidney Disease cohort. *Clin J Am Soc Nephrol* 1: 64–69, 2006
8. Hartigan JA, Wong MA: Algorithm AS 136: A K-means clustering algorithm. *J R Stat Soc Ser C Appl Stat* 28: 100–108, 1979
9. Sethian JA: Level set methods and fast marching methods, Cambridge, United Kingdom, Cambridge University Press, 1999
10. Weickert J: *Anisotropic diffusion in image processing*, Stuttgart, Teubner-Verlag, 1998
11. Malladi R, Sethian JA, Vemuri BC: Shape modeling with front propagation: a level set approach. *IEEE Trans Pattern Anal Mach Intell* 17: 158–175, 1995
12. Soille P: *Morphological image analysis: principles and applications*, Heidelberg, Springer-Verlag, 2003
13. Shrout PE, Fleiss JL: Intraclass correlations: Uses in assessing rater reliability. *Psychol Bull* 86: 420–428, 1979
14. Bland JM, Altman DG: Statistical methods for assessing agreement between two methods of clinical measurement. *Lancet* 1: 307–310, 1986
15. Torres VE, Chapman AB, Devuyst O, Gansevoort RT, Grantham JJ, Higashihara E, Perrone RD, Krasa HB, Ouyang J, Czerwiec FS; TEMPO 3:4 Trial Investigators: Tolvaptan in patients with autosomal dominant polycystic kidney disease. *N Engl J Med* 367: 2407–2418, 2012
16. Cadnapaphornchai MA, Masoumi A, Strain JD, McFann K, Schrier RW: Magnetic resonance imaging of kidney and cyst volume in children with ADPKD. *Clin J Am Soc Nephrol* 6: 369–376, 2011
17. Shim H, Chang S, Tao C, Wang JH, Kaya D, Bae KT: Semi-automated segmentation of kidney from high-resolution multi-detector computed tomography images using a graph-cuts technique. *J Comput Assist Tomogr* 33: 893–901, 2009
18. Khalifa F, Elnakib A, Beache GM, Gimel'farb G, El-Ghar MA, Ouseph R, Sokhadze G, Manning S, McClure P, El-Baz A: 3D kidney segmentation from CT images using a level set approach

guided by a novel stochastic speed function. *Med Image Comput Comput Assist Interv* 14: 587–594, 2011
19. Bae KT, Grantham JJ: Imaging for the prognosis of autosomal dominant polycystic kidney disease. *Nat Rev Nephrol* 6: 96–106, 2010

Received: October 17, 2012 **Accepted:** February 7, 2013

Present Address: Dr. Kyungsoo Bae, Department of Radiology, Gyeongsang National University School of Medicine, Jinju, South Korea.

Published online ahead of print. Publication date available at www.cjasn.org.